

Critical behavior in the layered organic-inorganic hybrid $(CH_3NH_3)_2CuCl_4$

Tina Raoufi, Yinina Ma(马怡妮娜), Young Sun(孙阳)

Citation: Chin. Phys. B . 2020, 29(6): 067503 . **doi:** 10.1088/1674-1056/ab892c
Journal homepage: http://cpb.iphy.ac.cn; http://iopscience.iop.org/cpb

What follows is a list of articles you may be interested in

Magnetocaloric effect and critical behavior of the Mn-rich itinerant material Mn_3GaC with enhanced ferromagnetic interaction

Pengfei Liu(刘鹏飞), Jie Peng(彭杰), Mianqi Xue(薛面起), Bosen Wang(王铂森)

Chin. Phys. B . 2020, 29(4): 047503 . **doi:** 10.1088/1674-1056/ab7da1

Computational study of inverse ferrite spinels

A EL Maazouzi, R Masrour, A Jabar, M Hamedoun

Chin. Phys. B . 2019, 28(5): 057504 . **doi:** 10.1088/1674-1056/28/5/057504

Magnetocaloric effect in the layered organic-inorganic hybrid $(CH_3NH_3)_2CuCl_4$

Yinina Ma(马怡妮娜), Kun Zhai(翟昆), Liqin Yan(闫丽琴), Yisheng Chai(柴一晟), Dashan Shang(尚大山), Young Sun(孙阳)

Chin. Phys. B . 2018, 27(2): 027501 . **doi:** 10.1088/1674-1056/27/2/027501

Magnetic transition and large reversible magnetocaloric effect in $EuCu_{1.75}P_2$ compound

Huo De-Xuan, Liao Luo-Bing, Li Ling-Wei, Li Miao, Qian Zheng-Hong

Chin. Phys. B . 2013, 22(2): 027502 . **doi:** 10.1088/1674-1056/22/2/027502

Mean-field and high temperature series expansion calculations of some magnetic properties of Ising and XY antiferromagnetic thin-films

R. Masrour, M. Hamedoun, A. Benyoussef

Chin. Phys. B . 2012, 21(8): 087503 . **doi:** 10.1088/1674-1056/21/8/087503

Critical behavior in the layered organic–inorganic hybrid $(CH_3NH_3)_2CuCl_4$*

Tina Raoufi[1,2], Yinina Ma(马怡妮娜)[1,2], and Young Sun(孙阳)[1,2,†]

[1] *Beijing National Laboratory for Condensed Matter Physics, Institute of Physics, Chinese Academy of Sciences, Beijing* 100190, *China*
[2] *School of Physical Sciences, University of Chinese Academy of Sciences, Beijing* 100190, *China*

(Received 13 March 2020; revised manuscript received 9 April 2020; accepted manuscript online 15 April 2020)

The critical properties and the nature of the ferromagnetic–paramagnetic phase transition in the 2D organic-inorganic hybrid $(CH_3NH_3)_2CuCl_4$ single crystal have been investigated by dc magnetization in the vicinity of the magnetic transition. Different techniques were used to estimate the critical exponents near the ferromagnetic–paramagnetic phase transition such as modified Arrott plots, the Kouvel–Fisher method, and the scaling hypothesis. Values of $\beta = 0.22$, $\gamma = 0.82$, and $\delta = 4.4$ were obtained. These critical exponents are in line with their corresponding values confirmed through the scaling hypothesis as well as the Widom scaling relation, supporting their reliability. It is concluded that this 2D hybrid compound possesses strong ferromagnetic intra-layer exchange interaction as well as weak interlayer ferromagnetic coupling that causes a crossover from 2D to 3D long-range interaction.

Keywords: critical behavior, critical exponent, organic-inorganic hybrid

PACS: 75.40.Cx, 75.50.–y **DOI:** 10.1088/1674-1056/ab892c

1. Introduction

Hybrid organic-inorganic compounds are an attractive family of materials in condensed matter physics, which have been extensively studied over the past decade for both fundamental science and technological applications.[1–5] Because of the combination of organic and inorganic moieties within a single structure, a variety of interesting properties have been discovered in these compounds.[6,7] In some organic-inorganic hybrids, the inorganic atoms are connected through covalent and ionic interactions to form the inorganic network. Meanwhile, the organic blocks can be connected by weaker interactions such as hydrogen and van der Waals bonding. Thus, a layered structure with quasi-two-dimensional magnetic interaction can be realized in them. Recently, two-dimensional (2D) magnetism has been a hot topic. It was previously thought that the surviving of long-range ferromagnetic (FM) order in 2D was hard due to increased fluctuation. However, the magnetic anisotropy in 2D magnetic crystals could stabilize the long-range magnetic order.[8]

To investigate the 2D magnetic phenomena, a critical exponent survey provides rich information. Accordingly, by evaluating the critical behavior, the nature of magnetic phase transition and inherent characteristics can be determined.[9]

Since the critical phenomena of magnetic organic-inorganic hybrids have not yet been well studied, in this paper, we performed a study on the critical behavior of a layer-structured organic-inorganic hybrid, $(CH_3NH_3)_2CuCl_4$. Various methods were used to estimate the critical exponents near the ferromagnetic–paramagnetic phase transition. A crossover from 2D to 3D long-range order was identified based on the analysis of the obtained critical exponents.

2. Experimental method

Single crystal samples of $(CH_3NH_3)_2CuCl_4$ were prepared via a solvothermal condition method as reported previously.[10] The structural properties of the samples were studied by x-ray diffraction using a Cu-$K\alpha$ radiation source. Direct-current (dc) magnetization was measured by using a Quantum Design magnetic properties measurement system (MPMS) with the magnetic field applied parallel to the metal-halogen layers.

3. Scaling analysis on the magnetization data

When a magnetic material undergoes a second-order phase transition, the critical behavior around Curie temperature T_C can be characterized by a series of interrelated critical exponents, namely, β, γ, and δ.[11]

The magnetic equations can be given as

$$M_S(T) = M_0(-\varepsilon)^{\beta}, \quad \varepsilon < 0, \quad T < T_C, \tag{1}$$

$$\chi_0^{-1}(T) = \left(\frac{h_0}{M_0}\right)(-\varepsilon)^{\gamma}, \quad \varepsilon > 0, \quad T > T_C, \tag{2}$$

$$M = DH^{1/\delta}, \quad \varepsilon = 0, \quad T = T_C, \tag{3}$$

where M_S is the spontaneous magnetization associated with β, χ_0^{-1} is the initial magnetic susceptibility associated with γ,

*Project supported by the National Natural Science Foundation of China (Grant No. 51725104) and the Beijing Natural Science Foundation, China (Grant No. Z180009).

†Corresponding author. E-mail: youngsun@iphy.ac.cn

© 2020 Chinese Physical Society and IOP Publishing Ltd

$\varepsilon = (T - T_C)/T_C$ is the reduced temperature associated with δ, and M_0, h_0, and D are the critical amplitudes.

The parameter β (in the region below T_C) is controlled by the temperature dependence of the spontaneous magnetization, and the parameter γ (in the region above T_C) is controlled by the temperature dependence of the initial susceptibility. At T_C, the δ exponent demonstrates the field dependence of the magnetization.

The scaling hypothesis provides another way to determine the critical exponents. The reduced magnetic equation of state that follows the critical region theory can be expressed as

$$M(H\varepsilon) = \varepsilon^{\beta} f_{\pm}(H/\varepsilon^{\beta+\gamma}), \tag{4}$$

where f_+ for $T > T_C$ and f_- for $T < T_C$.

The state described by the above equations will fall on two universal curves: one above T_C and the other below T_C. This is an important criterion for the critical regime; the exponents in the vicinity of T_C confirm the universal properties.

4. Results and discussion

Figure 1(a) displays crystal structure of $(CH_3NH_3)_2CuCl_4$. The octahedral complexes are sandwiched between organic blocks. It has been deduced that the diffraction peaks of the sample are in accord with the monoclinic perovskite structure with $P21/a$, the details of which were reported in Ref. [10]. Figure 1(b) displays the temperature dependence of magnetization under field cooled (FC) conditions with different applied magnetic fields in the *ab* plane of $(CH_3NH_3)_2CuCl_4$. The sample displays a FM–paramagnetic (PM) transition at $T_C \sim 9$ K in 0.1 T magnetic field, and the transition temperature shifts to a higher temperature with increasing magnetic field.

To determine the nature of the FM–PM phase transition, we plot the M^2 vs. H/M curves in Fig. 2(a). According to the criterion set by Banerjee,[12] the positive slope for the full range of temperatures and fields studied indicates a second-order phase transition. In this sample, the slope is positive and accordingly, the FM–PM phase transition is second order.

In order to gain a deeper insight into the mechanism of magnetic interactions between the spins during the magnetic phase transition, the critical exponents need to be analyzed.[13] We use the modified Arrott plots (MAPs) method based on the Arrott–Noaks state equation to obtain the precise values of the critical exponents and the class of universality to which $(CH_3NH_3)_2CuCl_4$ could belong. The isotherm magnetization data is transmitted to a sequence of $M^{1/\beta} = f(\mu_0 H/M)^{1/\gamma}$ curves.

According to this method, the MAP is analyzed by certain types of possible exponents belonging to the tricritical mean-field model ($\beta = 0.25$ and $\gamma = 1$), 3D-Heisenberg model ($\beta = 0.365$ and $\gamma = 1.336$), 3D-Ising model ($\beta = 0.325$ and $\gamma = 1.24$), and mean-field model ($\beta = 0.5$ and $\gamma = 1$), while the 2D-Ising model ($\beta = 0.125$ and $\gamma = 1.75$) is also considered,[11] which are shown in Figs. 2(b)–2(f).

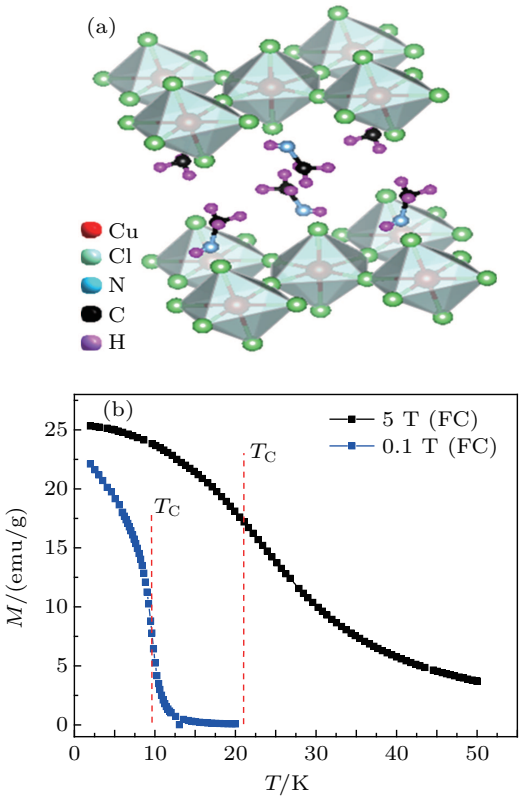


Fig. 1. (a) The crystal structure of the 2D organic-inorganic hybrid compound. (b) Temperature dependence of FC magnetization with different applied magnetic fields in the *ab* plane.

Table 1. Comparison of critical exponents of $(CH_3NH_3)_2CuCl_4$ obtained with different theoretical models: modified Arrott plot (MAP), Kouvel–Fisher (KF), critical isotherm analysis (CI).

	β	γ	δ
Mean-field	0.5	1	3
3D-Heisenberg	0.365	1.336	4.8
Triciritical mean-field	0.25	1	5
3D-Ising	0.325	1.24	4.82
2D-Ising	0.125	1.75	15
This work (MAP)	0.22	0.82	4.72
This work (KF)	0.22	0.81	4.68
This work (CI)			4.4

The critical exponents for the above-mentioned models have been predicted by particular values. The mean-field model is suitable to describe the long-range magnetic interaction, which is equivalent to the classic Landau model. The tritical mean-filed model is used to explain the first-order and second-order magnetic interactions of the magnetic phase transition. 3D-Ising is appropriate for understanding the magnetic anisotropic uniaxial magnetocrystalline interaction[14] and 3D-Heisenberg is suitable for investigating the short-range magnetic interaction. The critical behavior is impressively influenced by the magnetization data in high magnetic field regions due to interplay variables such as charge, lattice, and

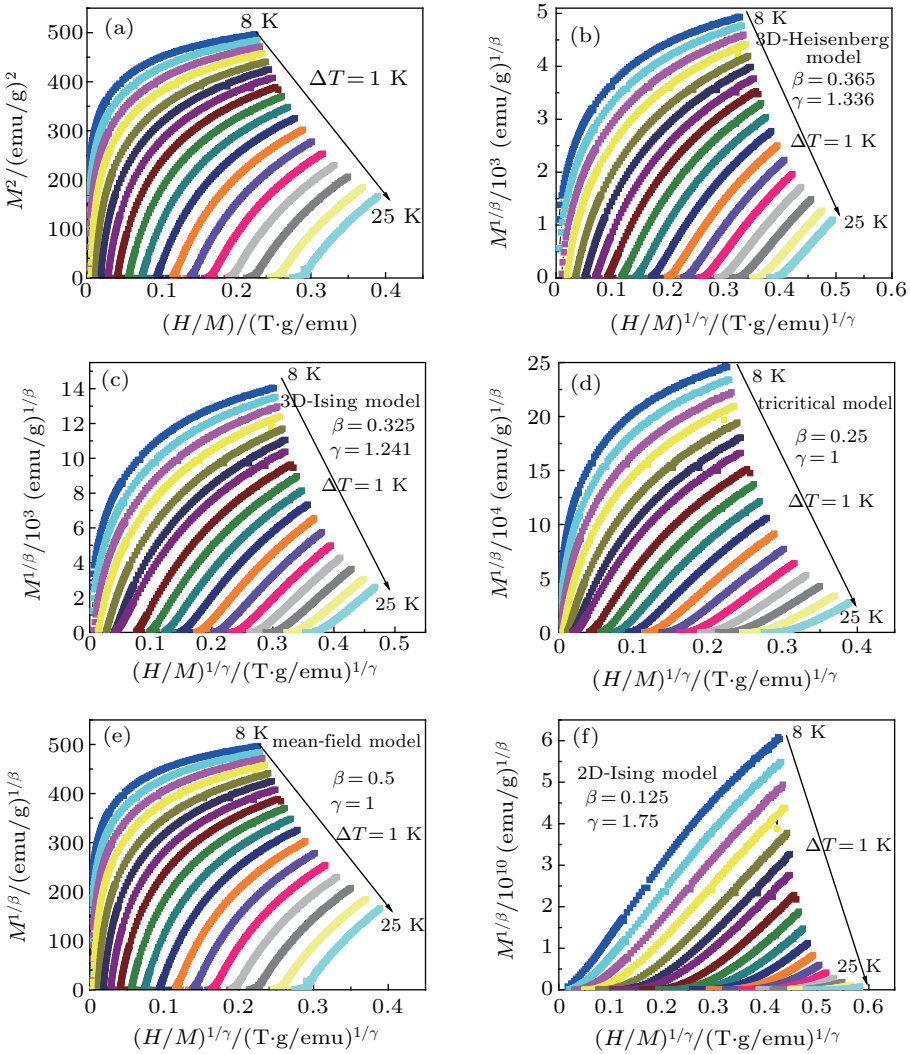


Fig. 2. (a) The Arrott plots of M^2 vs. H/M. (b)–(f) The modified Arrott plots with various models.

orbital degree of freedom in a ferromagnetic system.[15] The lower-field data have not been considered in the fitting process, because they represent the arrangement of magnetic domains.[16]

As seen in Figs. 2(b)–2(f), these curves display almost straight lines in the high-field regime. It is therefore difficult to identify the best model. In order to solve this problem, we calculate their relative slopes (RS) defined as RS $= S(T)/S(T_C)$, where $S(T)$ and $S(T_C)$ are the MAP slopes at temperatures T and T_C, respectively. The RS of the most appropriate model should be close to the optimal unity value.

Figure 3 shows the RS vs. T plots using the five distinct models. It demonstrates that the system is well defined by the tricritical mean-field model. The chosen exponents have $\beta = 0.25$ and $\gamma = 1$ as the initial values.

By following a standard procedure to identify the exact critical exponents β and γ, the linear extrapolation from the high-field straight line portions of the isotherms to the $M^{1/\beta}$ and $(\mu_0 H/M)^{1/\gamma}$ axes provides the spontaneous magnetization $M_S(T,0)$ and the initial susceptibility $\chi_0^{-1}(T,0)$, respectively. By fitting the data of $M_S(T,0)$ and $\chi_0^{-1}(T,0)$ following Eqs. (1) and (2), a set of β and γ can be obtained. Then, the obtained new critical exponents are used to repeat this procedure until convergence is reached and the values of β and γ are stable. The intersection of the linear extrapolation of the $M_S(T)$ and $\chi_0^{-1}(T)$ straight lines gives the value of T_C. The final values of the critical exponents generated are $\beta = 0.22$ and $\gamma = 0.82$, as depicted in Fig. 4.

Alternatively, the critical exponents and T_C can be specified more accurately by the Kouvel–Fisher (KF) method based on the following equations:

$$\frac{M_S(T)}{\mathrm{d}M_S(T)/\mathrm{d}T} = \frac{T - T_C}{\beta}, \tag{5}$$

$$\frac{\chi_0^{-1}(T)}{\mathrm{d}\chi_0^{-1}(T)/\mathrm{d}T} = \frac{T - T_C}{\gamma}. \tag{6}$$

According to this method, these equations are linear functions of temperature with slopes $1/\beta$ and $1/\gamma$, respectively.

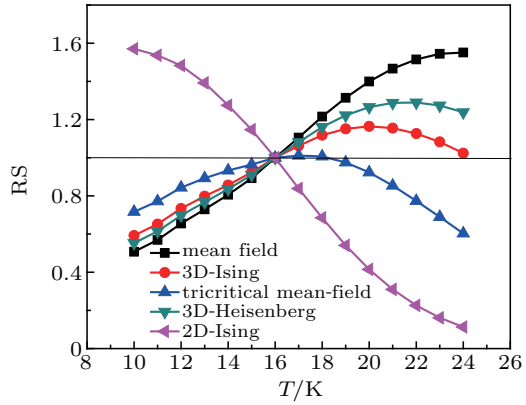


Fig. 3. Temperature dependence of the normalized relative slope for different models.

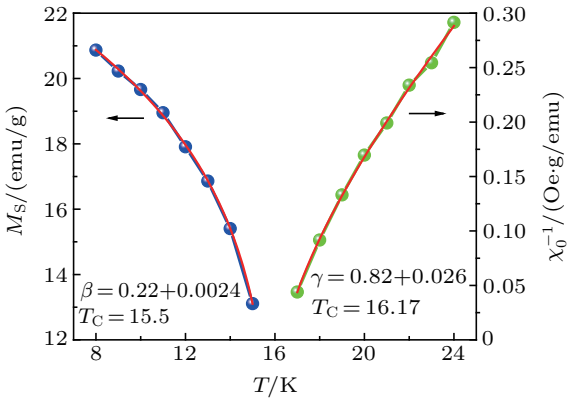


Fig. 4. Temperature dependence of the spontaneous magnetization M_S and the inverse susceptibility χ_0^{-1}.

As seen in Fig. 5, the new exponents of the linear fits are obtained as $\beta = 0.22$ with $T_C = 15.52$ and $\gamma = 0.82$ with $T_C = 15.93$, respectively. It is worthy to note that the values of the critical exponents and T_C deduced from the KF method agree with the estimation from the MAP technique.

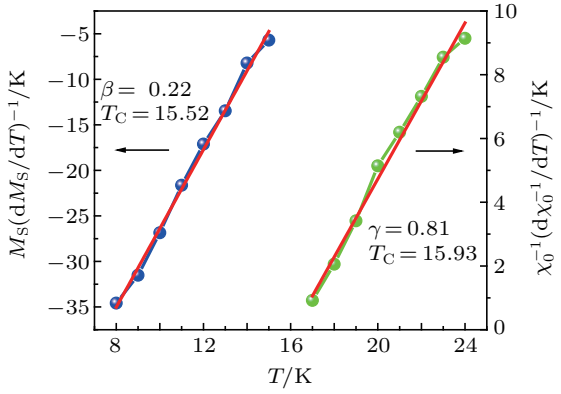


Fig. 5. The KF plots of M_S and χ_0^{-1}.

The third critical exponent δ can be calculated directly from the fitting of the critical isotherm M vs. H at T_C (Fig. 6(a)). According to Eq. (3), the high-field region of the critical isotherm at $T = 16$ K in log–log plot would give a solid straight line with a slope of $1/\delta$ (Fig. 6(b)). Subsequently, the δ exponent is obtained as 4.4.

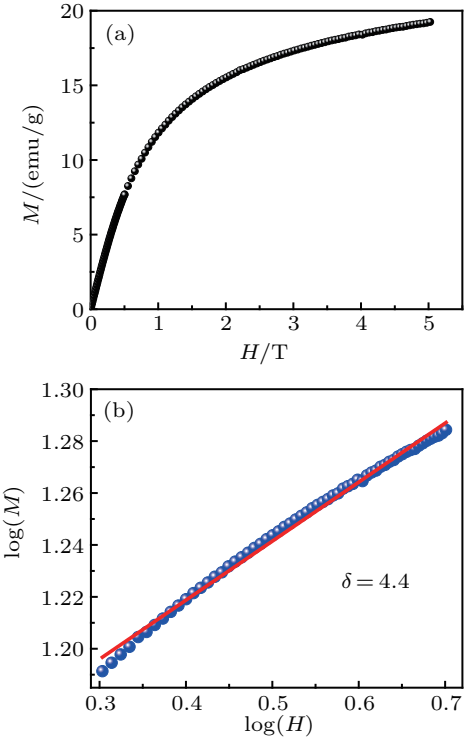


Fig. 6. (a) Isothermal $M(h)$ curve at T_C. (b) The same plot on a log–log scale. The straight line is the linear fit of Eq. (3).

According to Wisdom's scaling relation, the exponent δ can also be theoretically verified by the following relationship:

$$\delta = 1 + \frac{\gamma}{\beta}. \tag{7}$$

Based on the β and γ values obtained from the MAP, KF methods and Eq. (7), a value of 4.68 is obtained for δ. We emphasize that the values obtained from the critical isotherms and Widom's scaling are close. Thus, the critical exponents calculated in this research are accurate and self-consistent.

Since the obtained exponents of the sample are not matched with conventional universal classes, we investigate whether the acquired values of the critical exponents can generate the equation of the Widom's scaling or not.[15,17]

The scaling analysis of Eq. (4) can be used in the critical region to further confirm the validity of the results obtained so far and is calculated with the obtained critical exponents. The scaling equation implies that M/ε^{β} vs. $H/\varepsilon^{\beta+\gamma}$ yields two universal curves for $T > T_C$ and $T < T_C$, respectively.

Figure 7(a) shows that the experimental data collapse into two separate branches, one below T_C and the other above T_C. Figure 7(b) illustrates the same plots on the log–log scale. The experimental data collapse in the higher-field region into two distinct curves. This supports the validity of the obtained values of the critical exponents and T_C. However, while the scaling is effective in the high magnetic field regime, a tiny divergence is present in the low magnetic field regime. This can be attributed to the magnetic inhomogeneity. FM clusters may generate a local anisotropic field. When an applied field is not sufficiently high to overcome the local anisotropic field, the

magnetic moment can be aligned with a local anisotropic field. As a result, some magnetization data points do not entirely fall on the branches.[18,19]

The Arrott–Noakes equation of state is

$$\left(\frac{H}{M}\right)^{1/\gamma} = \left(\frac{T-T_{\rm C}}{T_{\rm C}}\right) + \left(\frac{M}{M_1}\right)^{1/\beta}, \tag{8}$$

where M_1 is constant and this equation of state is only obeyed at the limit of $T_{\rm C}$. The Arrott–Noakes equation is rewritten as[20]

$$\left(\frac{H}{M}\right)^{1/\gamma} = A' + B'(M)^{1/\beta}, \tag{9}$$

where A' and B' are temperature-dependent coefficients. Figure 8(a) depicts the $(H/M)^{1/\gamma}$ vs. $(M)^{1/\beta}$ curves constructed with the critical exponents obtained from the KF method. As can be seen, the set of lines are parallel to each other and the line at $T = T_{\rm C}$ passes through the origin. The line fitted by Eq. (9) and A', B' are shown in Fig. 8(b). It is notable that $T_{\rm C}$ is placed at the zero point of the perpendicular axis and the minimum of B' is placed at $T_{\rm C}$. The well-rescaled curves suggest that the obtained critical exponents are reliable.

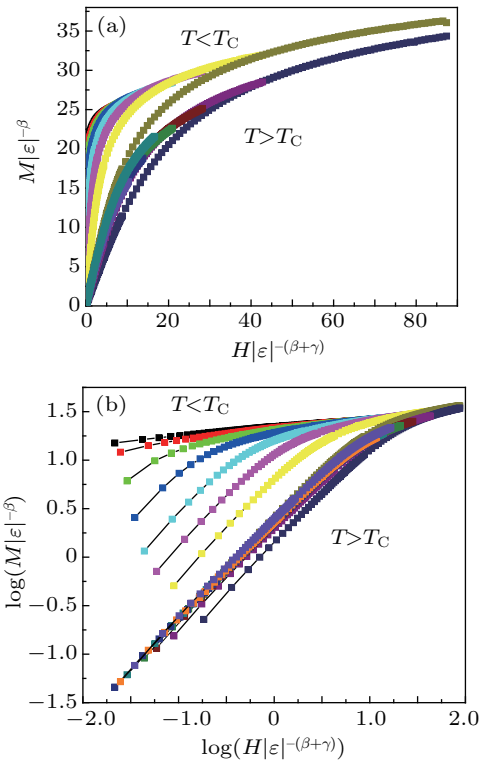


Fig. 7. (a) Scaling plots of renormalized magnetization $M|\varepsilon|^{-\beta}$ vs. $H|\varepsilon|^{-(\beta+\gamma)}$ using β and γ determined by the KF method. (b) The alternative plot on a log–log scale.

The obtained critical exponents in the present study do not belong to any predicted class of universality. The effective critical exponents ($\beta_{\rm eff}$ and $\gamma_{\rm eff}$) have been examined as a function of ε using Eq. (9) in order to determine whether they match any universality class in the asymptotic area of the system,

$$\beta_{\rm eff}(\varepsilon) = \frac{{\rm d}[\ln M_{\rm S}(\varepsilon)]}{{\rm d}[\ln \varepsilon]}, \quad \gamma_{\rm eff}(\varepsilon) = \frac{{\rm d}[\ln \chi_0^{-1}(\varepsilon)]}{{\rm d}[\ln \varepsilon]}. \tag{10}$$

The effective exponents $\gamma_{\rm eff}$ and $\beta_{\rm eff}$ as a function of reduced temperature ε are plotted in Fig. 9. Both $\beta_{\rm eff}$ and $\gamma_{\rm eff}$ show non-monotonic temperature dependence and do not match with any predicted universality class. A similar phenomenon was observed in many magnetic crystals.[21] This behavior is attributed to two sources: (1) spin disorder which restrains the rapid development of the FM state; (2) the crossover from 2D to 3D magnetic order. The disorder may arise from the inhomogeneous phase above and below $T_{\rm C}$.[22] According to the Harris criterion, if the heat capacity critical exponent is positive ($\alpha > 0$), the disorder changes the critical exponent. Meanwhile, if α is negative, the disorder is irrelevant.[23] Using the Rushbrooke scaling relation, which is given by[22] $\alpha + 2\beta + \gamma = 2$, the exponent α is found to be positive for the system, which implies that the disorder is relevant.

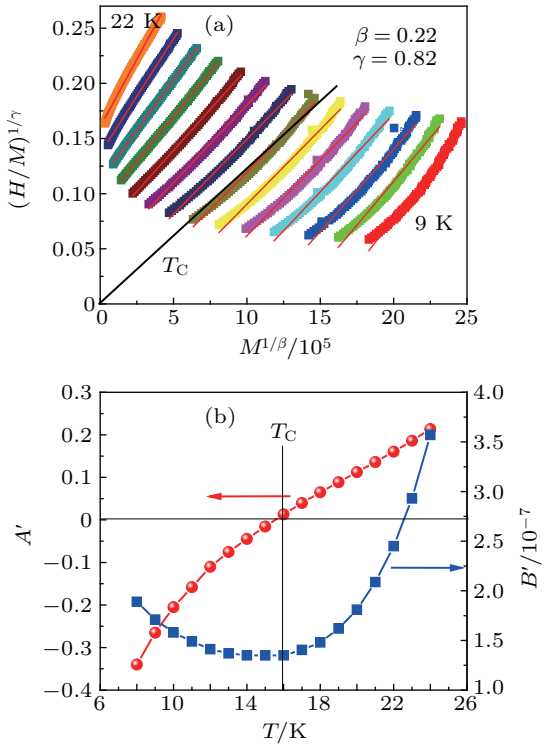


Fig. 8. (a) The $(H/M)^{1/\gamma}$ vs. $(M)^{1/\beta}$ curves with the critical exponents obtained from the KF method. (b) Temperature dependence of modified coefficients A' and B'.

The origin of the FM interaction in this compound is due to the magnetic ions (Cu) in the *ab* plane and the antiferro distortive displacement of the halide ions within the *ab* plane, which is the consequence of Jahn–Teller distortion of the octahedral complex in the inorganic sheet. As a result, the single unpaired electron is located in the $d_{x^2-y^2}$ orbital at each of the 3D holes of the Cu^{2+} ions in this compound, which aligns with the long axis of the octahedron and the spins experience FM superexchange, leading to a long-range FM order.[2,24–26]

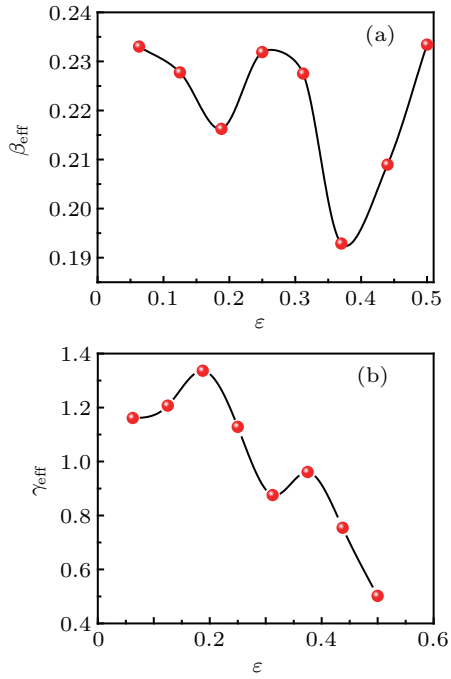


Fig. 9. Effective critical exponents (a) $\beta_{\rm eff}$ and (b) $\gamma_{\rm eff}$ as a function of the reduced temperature ε.

It is clear from the previous sections that the FM interaction in this system does not completely conform to any predictive model. The results from the report of Taroni *et al.* show that the critical exponent β for the bidimensional system should be within the range $0.1 \leq \beta \leq 0.25$.[26] The spontaneous survey magnetization by Jongh *et al.* illustrates that the critical exponent β is approximately 0.125 for the 2D system, except in the region very close to the ordering temperature; β will be changed to the 3D value of approximately 0.33 according to Griffiths universality hypothesis.[27] The β value of $(CH_3NH_3)_2CuCl_4$ is close to 0.25; this value lies between those of the 2D and 3D characteristics, which indicates that the interlayer coupling should be considerable. The exchange in the layer and between layers is typically strong and weak, respectively. Namely, the intralayer exchange is FM while the interlayer coupling is antiferromagnetic. For this sort of material including anisotropic intralayer exchange, a 2D-type behavior is predicted, but in a narrow ordering temperature (near $T_{\rm C}$), the crossover from 2D to 3D caused by the interlayer interaction begins to take effect.[28] The γ value is close to the mean-field model prediction and δ is located between the long-range and short-range couplings. These exponents can be attributed to a crossover effect of the 2D to the 3D system. To describe the crossover effect, we should consider the interlayer coupling.

The results indicate that the critical exponents in this compound do not strictly belong to the common universality models. Accordingly, it is important to determine the nature and the range of the interaction in the present study. For a homogeneous magnetic system, the universality of the magnetic phase transition is strongly dependent on the exchange interaction $J(r)$. Renormalization group theory treats the magnetic ordering as an attractive interaction of spin which decays with distance r as

$$J(r) = r^{-(d+\sigma)}, \tag{11}$$

where d is the spatial dimension and σ is the range of interaction. Moreover, the susceptibility exponent σ is predicted as

$$\gamma = 1 + \frac{4}{d}\left(\frac{n+2}{n+8}\right)\Delta\sigma + \frac{8(n+2)(n-4)}{d^2(n+8)^2} \times \left[1 + \frac{2G(d/2)(7n+20)}{(n-4)(n+8)}\right]\Delta\sigma^2, \tag{12}$$

where $\Delta\sigma = (\sigma - d/2)$, $G(d/2) = 3 - \frac{1}{4}(d/2)^2$, and n is the spin dimensionality.

It has been argued that if $\sigma \geqslant 2$, the 3D-Heisenberg parameter is valid, where $J(r)$ decreases faster than r^{-5}. When $\sigma \leqslant 3/2$, the conditions for the mean-field model are satisfied so that $J(r)$ decreases more slowly than $r^{-4.5}$. In this research work, by using Eq. (12) we see that $\sigma = 122$ ($d = 3$, $n = 3$), so the exchange distance decays as $J(r) \approx r^{-4.22}$, in agreement with a long-range interaction.

The previous study of the field dependent susceptibility demonstrated a very weak FM coupling near $T_{\rm C}$ between the layers that causes the space dimensionality of the system to crossover to a 3D long-range order.[25] From the studies performed so far, it can be concluded that the strong magnetic anisotropy, as well as the dipole interaction and inevitable interlayer interaction, can induce the system to display a 3D long-range magnetic characteristic above $T_{\rm C}$.[29]

5. Conclusion

We have provided a detailed analysis on the critical exponents of the organic-inorganic hybrid with the formula $(CH_3NH_3)_2CuCl_4$. The system undergoes a second-order PM–FM phase transition. By using various methods, such as MAPs, Kouvel–Fisher, and critical isotherm analysis, the reliable critical exponents of $\beta = 0.22$, $\gamma = 0.82$, and $\delta = 4.4$ were estimated. The critical exponents of this system do not belong to any universality class. The value of β is between those of the 2D and 3D systems and suggests a crossover from 2D to 3D near the Curie temperature.

References

[1] Zolfaghari P, De Wijs G A and De Groot R A 2013 *J. Phys.: Condens. Matter.* **25** 295502
[2] Day P 1985 *Phil. Trans. R. Soc. Lond. A* **314** 145
[3] Rao C N R, Cheetham A K and Thirumurugan A 2008 *J. Phys: Condens. Matter.* **20** 083202
[4] Li W, Wang Z, Deschler F, Gao S, Friend R H and Cheetham A K 2017 *Nat. Rev. Mater.* **2** 16099
[5] Ma Y, Cong J and Sun Y 2019 *J. Phys.: Condens. Matter.* **31** 205701

[6] Tian Y, Shen S, Cong J, Yan L, Wang S and Sun Y 2016 *J. Am. Chem. Soc.* **138** 782
[7] Tian Y, Stroppa A, Chai Y S, Barone P, Perez-Mato M, Picozzi S and Sun Y 2015 *Phys. Status Solidi.* **9** 62
[8] Gong C and Zhang X 2019 *Science.* **363** eaav4450
[9] Ghosh K, Lobb C J, Greene R L, Karabashev S G, Shulyatev D A, Arsenov A A and Mukovskii Y 1998 *Phys. Rev. Lett.* **81** 4740
[10] Ma Y, Zhai K, Yan L, Chai Y, Shang D and Sun Y 2018 *Chin. Phys. B* **27** 027501
[11] Liu Y and Petrovic C 2017 *Phys. Rev. B* **96** 054406
[12] Banerjee B K 1964 *Phys. Lett.* **12** 16
[13] Ameur N, Triki M, Dhahri E and Hlil E K 2019 *Solid State Commun.* **292** 40
[14] Hou K Y, Dong Q Y, Su L, Zhang X Q and Cheng Z H 2019 *J. Alloy. Compd.* **788** 155
[15] EhsaniM H and Raoufi T 2018 *J. Alloy. Compd.* **769** 649
[16] Lin G T, Zhuang H L, Luo X, Liu B J, Chen F C, Yan J, Sun Y, Zhou J, Lu W J, Tong P and Sheng Z G 2017 *Phys. Rev. B* **95** 245212
[17] Li R, Zhang C, Pi L and Zhang Y 2014 *EPL.* **107** 47006
[18] Phan T L, Zhang Y D, Zhang P, Thanh T D and Yu S C 2012 *J. Appl. Phys.* **112** 093906
[19] Dupas A and Renard J P 1975 *Phys. Lett. A* **53** 141
[20] Zhang L, Wang B, Sun Y, Tong P, Fan J, Zhang C, Pi L and Zhang Y 2012 *Phys. Rev. B* **85** 104419
[21] Perumal A, Srinivas V, Rao V, Dunlap R 2003 *Phys. Rev. Lett.* **91** 137202
[22] Zarai E, Issaoui F, Tozri A, Husseinc M and Dhahri E 2016 *J. Supercond. Nov. Magn.* **29** 869
[23] Dudka M, Folk R, Holovatch Y and Ivaneiko D 2003 *J. Magn. Magn. Mater.* **256** 243
[24] Liu Y and Petrovic C 2018 *Phys. Rev. B* **97** 014420
[25] Narita N and Yamada I 1996 *J. Phys. Soc. Jap.* **65** 4054
[26] Taroni A, Bramwell S T and Holdsworth P C 2008 *J. Phys: Condens. Matter.* **20** 275233
[27] de Jongh L J and Miedema A R 1974 *Adv. Phys.* **23** 1
[28] Rubenacker G V, Haines D N, Drumheller J E and Emerson K 1984 *J. Magn. Magn. Mater.* **43** 238
[29] Lin G T, Luo X, Chen F C, Yan J, Gao J J, Sun Y, Tong W, Tong P, Lu W J, Sheng Z G, Song W H, Zhu X B and Sun Y P 2018 *Appl. Phys. Lett.* **112** 072405